Stem Cell Reports
Article

OPEN ACCESS

p53 and p73 Regulate Apoptosis but Not Cell-Cycle Progression in Mouse Embryonic Stem Cells upon DNA Damage and Differentiation

Hanbing He,[1,3] Cheng Wang,[1,3] Qian Dai,[2] Fengtian Li,[1] Johann Bergholz,[1] Zhonghan Li,[1] Qintong Li,[2,*] and Zhi-Xiong Xiao[1,*]

[1]Center of Growth, Metabolism and Aging, Key Laboratory of Bio-Resource and Eco-Environment, Ministry of Education, College of Life Sciences, Sichuan University, 19 Wang Jang Road, Chengdu 610064, China
[2]Department of Pediatrics, West China Second University Hospital, Key Laboratory of Birth Defects and Related Diseases of Women and Children (Sichuan University), Ministry of Education, Sichuan University, Chengdu 610041, China
[3]Co-first author
*Correspondence: jimzx@scu.edu.cn (Z.-X.X.), liqintong@scu.edu.cn (Q.L.)
http://dx.doi.org/10.1016/j.stemcr.2016.10.008

SUMMARY

Embryonic stem cells (ESCs) are fast proliferating cells capable of differentiating into all somatic cell types. In somatic cells, it is well documented that p53 is rapidly activated upon DNA damage to arrest the cell cycle and induce apoptosis. In mouse ESCs, p53 can also be functionally activated, but the precise biological consequences are not well characterized. Here, we demonstrated that doxorubicin treatment initially led to cell-cycle arrest at G2/M in ESCs, followed by the occurrence of massive apoptosis. Neither p53 nor its target gene p73 was required for G2/M arrest. Instead, p53 and p73 were fully responsible for apoptosis. p53 and p73 were also required for differentiation-induced apoptosis in mouse ESCs. In addition, doxorubicin treatment induced the expression of retinoblastoma protein in a p53-dependent manner. Therefore, both p53 and p73 are critical in apoptosis induced by DNA damage and differentiation.

INTRODUCTION

Embryonic stem cells (ESCs) are self-renewing pluripotent cells, derived from the inner cell mass of blastocyst (Smith, 2001). The transcriptional control of pluripotency is well characterized. Master transcription factors, such as *Pou5f1 (Oct4)*, *Sox2*, and *Nanog*, maintain pluripotency and suppress lineage-affiliated transcripts. Another distinct feature of ESCs is their fast proliferation rate with a much truncated G1 phase. Such characteristics impose a burden for ESCs to maintain genome stability. ESCs are hyper-sensitive to DNA damage, resulting in high levels of apoptosis (Hong and Stambrook, 2004; Qin et al., 2007). The molecular underpinnings are not well understood.

The molecular mechanisms that control ESC cell-cycle progression and genome stability may differ from those in somatic cells. For example, p53 is a well-known tumor suppressor and frequently mutated in cancer (Freed-Pastor and Prives, 2012; Isobe et al., 1986; Kruse and Gu, 2009). The major function of p53 is to maintain genome stability. In response to cellular stresses, p53 is stabilized and activated, resulting in cell-cycle arrest, apoptosis, or senescence by directly trans-activating downstream target genes such as *p21*, *Mdm2*, *Noxa*, and *Puma* (Vousden and Prives, 2009). However, the role of p53 in ESCs upon DNA damage is controversial, with some studies showing p53-dependent apoptosis while others show opposite results (Aladjem et al., 1998; de Vries et al., 2002). In addition, the role of the p53 protein family member, p73, is not clear in ESCs. The *Trp73* gene encodes two major isoforms, TAp73 andΔNp73, transcribed from alternative promoters (Sayan et al., 2010). TAp73 can induce cell death via trans-activation of target genes (Irwin et al., 2000), whereas the amino-terminal truncated ΔNp73 has an anti-apoptotic function (Nakagawa et al., 2002).

Retinoblastoma protein (RB) is a well-characterized tumor suppressor that negatively regulates G1/S transition in somatic cells. RB is highly expressed in ESCs but does not seem to be functional in affecting cell-cycle progression, presumably due to its hyper-phosphorylation. However, ESCs require the RB protein family to initiate the differentiation program (Conklin et al., 2012).

In this study, we show that doxorubicin induced dramatic G2/M cell-cycle arrest followed by massive apoptosis in mouse ESCs. Interestingly, cell-cycle G2/M arrest was not dependent on p53, p73, or RB. In contrast, both p53 and p73 proteins were required for doxorubicin-induced apoptosis. In addition, knockdown of either p53 or p73 significantly reduced differentiation-induced apoptosis. Notably, p53 also induced RB expression in ESCs likely via suppression of RB-targeting miRNAs. Together, these results suggest that p53 and p73 function to maintain genome stability in ESCs by inducing apoptosis upon DNA damage and differentiation.

RESULTS

Doxorubicin Induces Cell-Cycle Arrest and Apoptosis in Mouse Embryonic Stem Cells

In order to investigate the cellular response of mouse ESCs to DNA damage, we treated R1 mouse ESCs with

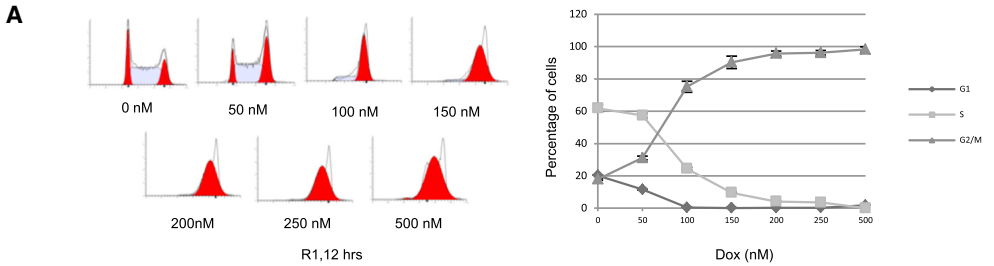

（nM）	0	50	100	150	200	250	500
G1(%):	20.3±0.2	11.6±0.3	0.4±0.2	0.2±0.1	0.2±0.1	0.3±0.1	1.8±0.6
S(%):	61.8±2.4	57.3±1.5	24.5±0.8	9.6±0.3	4.1±0.4	3.6±0.3	0.0
G2/M (%):	17.9±0.5	31.1±1.2	75.1±3.4	90.2±3.8	95.7±1.5	96.1±1.4	98.2±1.7

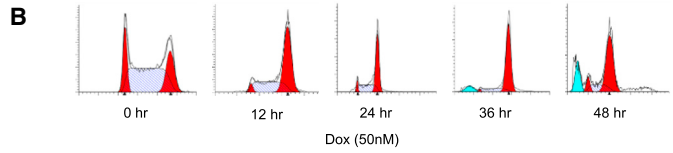

50nM/hrs	0 h	12 h	24 h	36 h	48 h
G1 (%):	18.3±0.4	3.9±0.2	3.1±0.4	1.6±0.3	9.2±1.1
S (%):	59.0±2.1	48.2±1.5	34.8±0.3	16.5±0.4	20.6±0.4
G2/M (%):	22.7±0.5	47.9±1.3	62.1±2.1	81.9±3.5	70.2±2.7
SubG1(%):	0.0	0.0	4.9±0.3	10.6±1.3	20.9±1.2

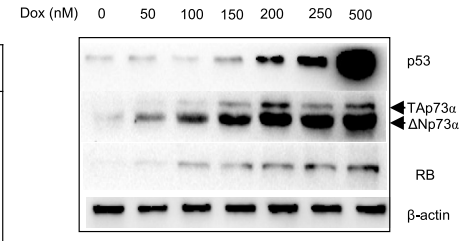

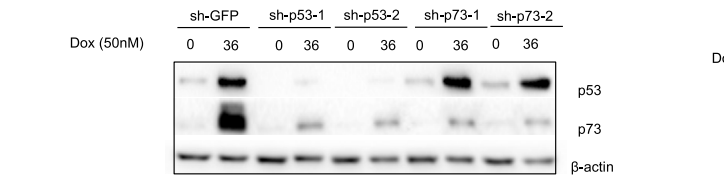

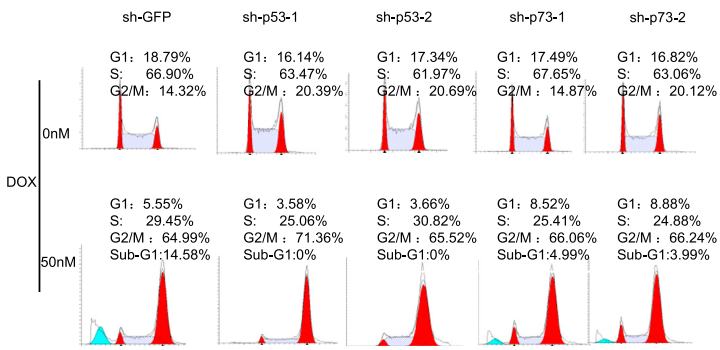

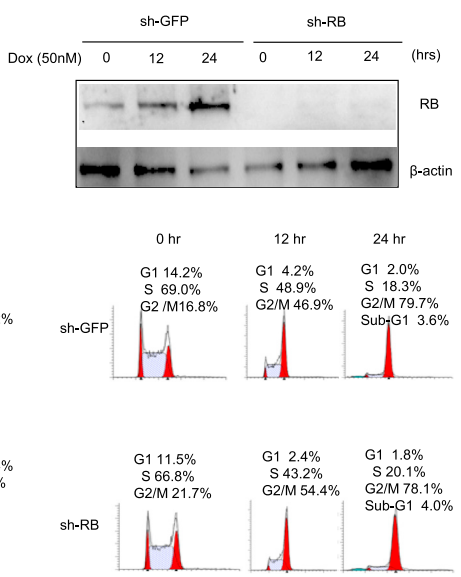

(legend on next page)

doxorubicin. As expected, R1 cells cultured under self-renewal conditions proliferated rapidly as demonstrated by a high percentage of S-phase cells. Treatment of doxorubicin for 12 hr induced G2/M cell-cycle arrest in a dose-dependent manner. Apparently, doxorubicin at a final concentration of 150 nM was effective to induce cell-cycle arrest at G2/M (Figure 1A). Notably, there was little sub-G1 cell population under these conditions (Figure 1A, bottom panel). To examine the effects of low-dose doxorubicin on cell-cycle progression, we treated R1 cells with 50 nM doxorubicin for up to 48 hr. As shown in Figure 1B, G2/M fractions of R1 cells were 47% at 12 hr, 62% at 24 hr, and 81% at 36 hr. At 48 hr, there was a significant sub-G1 population. Notably, cisplatin (CDDP) also induced G2/M arrest and apoptosis in R1 mouse ESCs (Figure S1). Similarly, doxorubicin also induced G2/M arrest and apoptosis in another mouse ESC line, AB2.2 (Figure S2).

We then analyzed the expression of p53, p73, and RB protein in mouse ESCs upon doxorubicin or CDDP. p53, p73, and RB protein levels were significantly increased upon treatment of doxorubicin (Figure 1C) or CDDP (Figure S1). Similarly, doxorubicin also induced p53, p73, and RB protein levels in AB2.2 mouse ESCs (Figure S2).

In order to investigate the role of p53, p73, and RB in doxorubicin-induced G2/M cell-cycle arrest, R1 cells stably expressing shRNA constructs specific for p53 (sh-p53-1, sh-p53-2) or p73 (sh-p73-1, sh-p73-2) (Johnson et al., 2007; Kawamura et al., 2009), as well as control cells (sh-GFP), were generated. As shown in Figure 1D, knockdown of p53 or p73 did not alter the cell-cycle profiles upon doxorubicin treatment, indicating that doxorubicin-induced G2/M cell-cycle arrest is independent of p53 or p73. Similarly, knockdown of RB had no significant effect on doxorubicin-induced G2/M arrest (Figure 1E).

We then investigated protein(s) that might be responsible for doxorubicin-induced G2/M arrest of R1 cells. It has been reported that ionizing radiation induces ATM-dependent G2/M arrest in human ESCs (Momcilovic et al., 2009). We treated R1 cells with 50 nM doxorubicin for either 12, 24, or 36 hr in the presence of KU55933, an ATM inhibitor (Qi et al., 2016). Consistent with previous reports (Hickson et al., 2004), inhibition of ATM reduced the level of p53 comparable with that in control cells (compare lane 5 with lane 1, Figure S3). However, inhibition of ATM did not alter G2/M arrest induced by doxorubicin (Figure S3).

p53 and p73 Are Critical in Doxorubicin-Induced Apoptosis in Mouse ESCs

We studied the time course of doxorubicin-induced cell-cycle arrest and apoptosis. As shown in Figure 2A, high-dose doxorubicin (250 nm) induced G2/M accumulation in R1 mouse ESCs in a time-dependent fashion, and reached a plateau at 12 hr after treatment, followed by the occurrence of apoptosis at 20 hr, and increased substantially at 24 hr. Thus, G2/M cell-cycle arrest preceded apoptosis. Western blot analyses showed that doxorubicin significantly increased expression of p53, preceding the increased expression of p73 and RB, and also cleaved caspase-3 in R1 and AB2.2 ESCs (Figures 2B and S2).

To investigate whether p53 and p73 regulate apoptosis in response to doxorubicin in ESCs, we generated ESC lines stably expressing short hairpin RNA specific for mouse p53 (sh-p53-1 and sh-p53-2), mouse p73 (sh-p73-1 and sh-p73-2) (Johnson et al., 2007; Kawamura et al., 2009), or GFP (sh-GFP) as a control. As shown in Figure 2C, knockdown of p53 completely abolished doxorubicin-induced apoptosis, whereas knockdown of p73 significantly, but not completely, reduced doxorubicin-induced apoptosis. Consistent with the fluorescence-activated cell sorting (FACS) data, western blot analyses confirmed that doxorubicin readily induced apoptosis, as

Figure 1. Doxorubicin Induces G2/M Arrest of R1 Cells Independently of p53, p73, or RB

R1 cells were treated with doxorubicin (Dox) at the indicated concentration for 12 hr and were then subjected to FACS analyses (A) or western blot analyses (C).

(A) Left: cell-cycle profiles. Right: percentages of cells in G1, S, and G2/M. Data are presented as means ± SE from three independent experiments.

(B) R1 cells were treated with 50 nM doxorubicin for the indicated time and then subjected to FACS analyses. At least three independent experiments were performed. Representative histograms are shown.

(C) Western blot analysis of p53, p73, and RB protein levels after different doses of doxorubicin treatment for 12 hr in R1 cells. β-Actin served as a loading control.

(D) Stable R1 cells expressing sh-GFP, sh-p53-1, sh-p53-2, sh-p73-1, or sh-p73-2 were treated with 50 nM doxorubicin for 36 hr, and cells were then subjected to western blot analyses or FACS analyses. At least three independent experiments were performed. Representative histograms and western blot data are shown.

(E) Stable R1 cells expressing sh-GFP or sh-RB were treated with 50 nM doxorubicin for 0, 12, or 24 hr and subjected to western blot analyses or FACS analyses. At least three independent experiments were performed. Representative histograms and western blot data are shown.

See also Figures S1–S3.

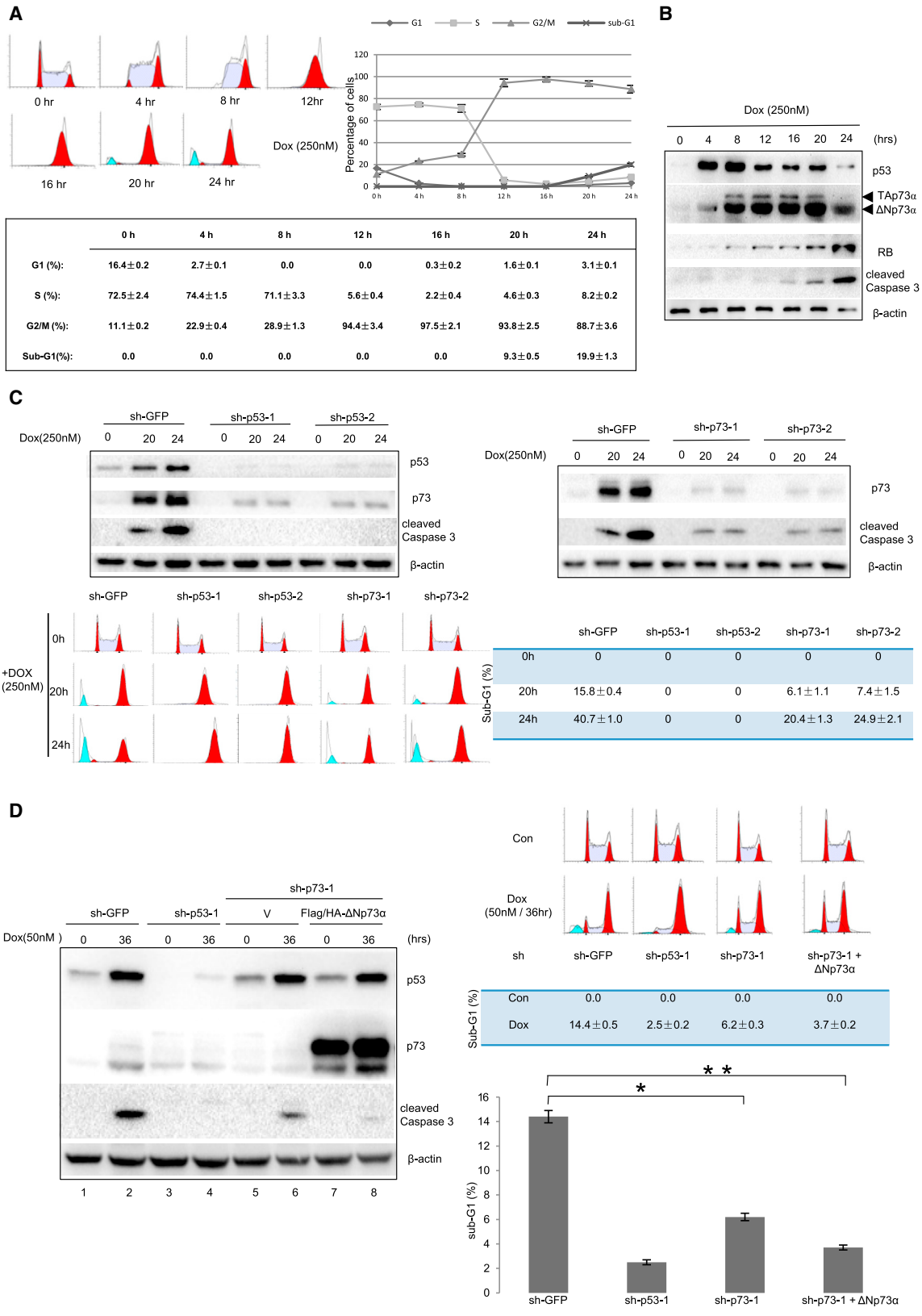

	0 h	4 h	8 h	12 h	16 h	20 h	24 h
G1 (%):	16.4±0.2	2.7±0.1	0.0	0.0	0.3±0.2	1.6±0.1	3.1±0.1
S (%):	72.5±2.4	74.4±1.5	71.1±3.3	5.6±0.4	2.2±0.4	4.6±0.3	8.2±0.2
G2/M (%):	11.1±0.2	22.9±0.4	28.9±1.3	94.4±3.4	97.5±2.1	93.8±2.5	88.7±3.6
Sub-G1(%):	0.0	0.0	0.0	0.0	0.0	9.3±0.5	19.9±1.3

Sub-G1 (%)	sh-GFP	sh-p53-1	sh-p53-2	sh-p73-1	sh-p73-2
0h	0	0	0	0	0
20h	15.8±0.4	0	0	6.1±1.1	7.4±1.5
24h	40.7±1.0	0	0	20.4±1.3	24.9±2.1

Sub-G1 (%)	sh-GFP	sh-p53-1	sh-p73-1	sh-p73-1 + ΔNp73α
Con	0.0	0.0	0.0	0.0
Dox	14.4±0.5	2.5±0.2	6.2±0.3	3.7±0.2

(legend on next page)

demonstrated by cleaved caspase-3 in control cells but not cells with knockdown of p53. Notably, re-introduction of human ΔNp73α in p73 knockdown cells almost completely inhibited doxorubicin-induced apoptosis (Figure 2D), suggesting that ΔNp73α functioned to inhibit apoptosis in response to doxorubicin.

Mouse ESCs have been shown to exist as a multiple state of pluripotency. Thus, we cultured R1 mouse ESCs in 2i/LIF conditions to induce cells to the naive state (Ying et al., 2008). As shown in Figure S4, as expected, naive R1 mouse ESCs exhibited a different morphology cell-cycle profile with a high percentage of G1 phase and a clear increase in the Nanog protein level and a decrease in c-MYC protein levels (Silva et al., 2009; Ying et al., 2008). Doxorubicin treatment of naive R1 mouse ESCs (sh-GFP) induced G2/M arrest and apoptosis. Similar to that of R1 cells grown in serum-containing media, effective knockdown of p53, as demonstrated by western blot analyses, did not affect doxorubicin-induced G2/M arrest, but it completely abolished apoptosis; again, knockdown of p73 did not affect doxorubicin-induced G2/M arrest but dramatically reduced apoptosis. Thus, our data indicate that p53 induces p73 expression, and both p53 and p73 play critical roles in apoptosis of both primed and naive-state mouse ESCs in response to doxorubicin.

p53 Upregulates p73 Transcription in Mouse ESCs in Response to Doxorubicin

Post-translational modification of p53 is critical in the regulation of p53 stability, cellular localization, and activity (Kruse and Gu, 2009). Indeed, doxorubicin dramatically induced p53 phosphorylation at Ser-18 (Figure 3A), a modification known to decrease the p53-MDM2 interaction, which leads to p53 protein accumulation and increased transcriptional activity (Chao et al., 2000). To demonstrate that p53 trans-activation activity in mouse ESCs is upregulated in response to doxorubicin, we performed real-time qPCR analyses. As shown in Figure 3B, doxorubicin significantly increased p21 and MDM2 mRNA levels but significantly reduced Nanog mRNA levels, consistent with a previous report that p53 negatively regulates Nanog expression (Lin et al., 2005). Notably, both p73 mRNA and protein levels were dramatically increased upon doxorubicin treatment in R1 mouse ESCs but not in p53 knockdown R1 mouse ESCs (Figure 3C). We concluded that doxorubicin upregulates p73 expression in a p53-dependent manner in mouse ESCs.

p53 Upregulates RB Protein Expression in Mouse ESCs in Response to Doxorubicin

Our aforementioned data demonstrated that both p53 and RB protein levels were increased significantly in response to doxorubicin (Figure 1B). We therefore examined whether p53 plays a role in doxorubicin-induced upregulation of RB expression. As shown in Figure 4A, again, in response to doxorubicin, RB protein expression was significantly increased in R1 mouse ESCs, but not in the cells with p53 knocked down. Real-time qPCR analyses showed that the RB mRNA levels were comparable in control cells and sh-p53-1 cells upon doxorubicin treatment (Figure 4B). These data suggest that p53-mediated regulation of RB is most likely at the post-transcriptional level.

It has been reported that miRNAs are potential regulators of RB protein translation. We used three algorithms, TargetScan, microRNA.org, and PicTar, to search for potential miRNA candidates that might regulate RB expression. The top candidates were miR-17, miR-20a, miR-106a, and miR-20b derived from the *mir-17-92* gene and *mir-106a-363* gene cluster (Mendell, 2008). These four miRNAs contain the same core sequence complementary to the 3′ UTR of mouse RB mRNA (Figure 4C). We therefore hypothesized that p53 likely suppresses expression of these miRNAs that resulted in upregulation of RB expression.

To explore this possibility, we performed real-time qPCR analyses to examine the expression of pri-miR-17-92 and pri-miR-106a-363 in R1 sh-GFP and R1 sh-p53-1 cells

Figure 2. High-Dose Doxorubicin Treatment Induces Apoptosis of R1 Cells in a p53-Dependent Manner

R1 cells were treated with 250 nM doxorubicin for the indicated time. Cells were then subjected to FACS analyses (A) or western blot analyses (B).

(A) Left: cell-cycle profiles. Right: percentages of cells in G1, S, G2/M, and sub-G1. Data are presented as means ± SE calculated from three independent experiments.

(B) Western blot analysis of p53, p73, RB, and cleaved caspase-3 protein levels after 250 nM doxorubicin treatment at the indicated time. β-Actin served as a loading control.

(C) Stable R1 cells expressing sh-GFP, sh-p53-1, sh-p53-2, sh-p73-1, or sh-p73-2 were treated with 250 nM doxorubicin at indicated time points and subjected to western blot analyses or FACS analyses. At least three independent experiments were performed. Representative histograms and western blot data are shown.

(D) R1 sh-p73 cells with ectopic expression of human ΔNp73α were treated with 50 nM doxorubicin for 36 hr and subjected to western blot analyses or FACS analyses. At least three independent experiments were performed. Representative histograms and western blot data are shown.

Data presented are means ± SE calculated from three independent experiments. *$p < 0.05$; **$p < 0.01$. See also Figures S1 and S4.

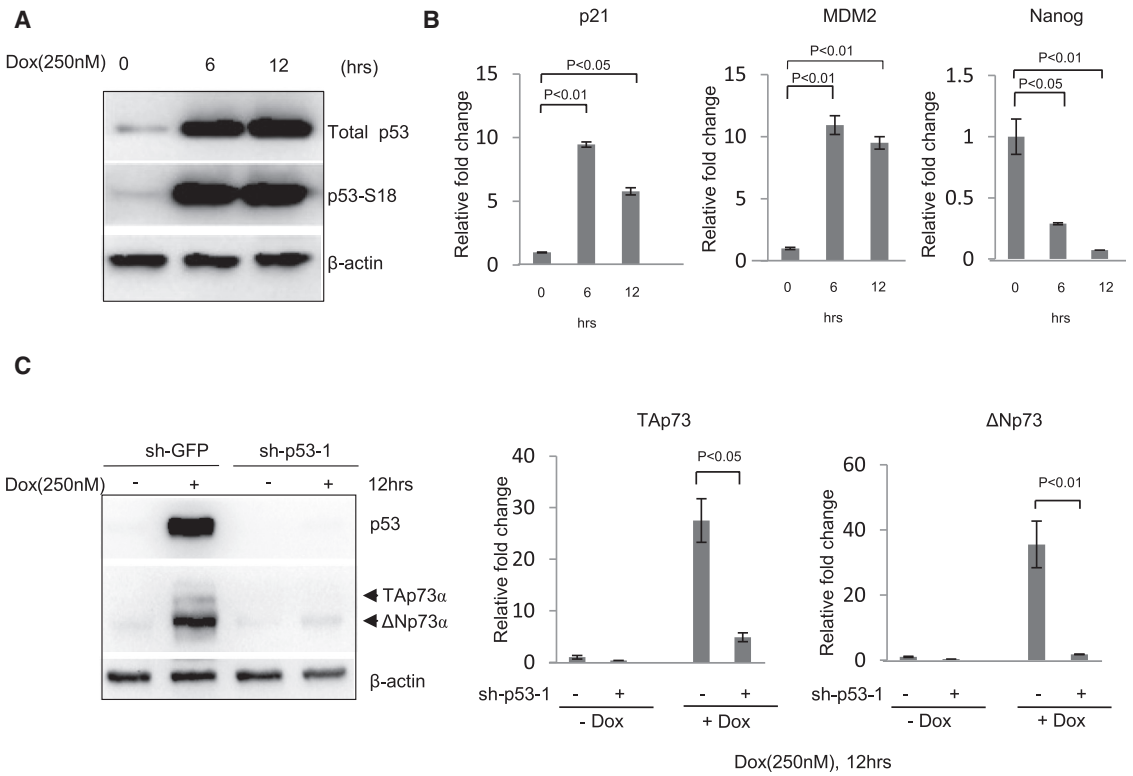

Figure 3. Doxorubicin Induces p73 Expression in R1 Cells in a p53-Dependent Manner

(A) R1 cells were treated with 250 nM doxorubicin for 6 or 12 hr. Western blot analyses for total p53 and phosphor-p53 (S18) were performed. β-Actin served as a loading control.

(B) R1 cells were treated with or without 250 nM doxorubicin for 6 or 12 hr. Total RNA was isolated and the expression of p53 downstream targets, p21, MDM2, and Nanog, were analyzed by qPCR. The changes in steady-state levels of mRNA (fold) were calculated using the $-\Delta\Delta C_t$ method and normalized using β-actin as a control. The mean of three independent experiments in triplicate are presented. Error bars represent SEM.

(C) R1 sh-GFP and R1 sh-p53-1 cells were treated with or without 250 nM doxorubicin for 12 hr and subjected to western blot analyses or qPCR analyses, as indicated. The steady-state levels of mRNA changes (fold) were calculated using the $-\Delta\Delta C_t$ method and normalized using β-actin as a control. The mean of three independent experiments in triplicate are presented. Error bars represent SEM.

upon doxorubicin treatment. Interestingly, the expression of pri-miR-17-92 and pri-miR-106a-363 was dramatically decreased in sh-GFP cells following DNA damage. However, the expression levels of these two miRNA clusters were largely comparable with p53 knockdown. Thus, it seemed that p53 likely upregulated RB expression via suppression of RB-targeting miRNAs.

Differentiation-Induced Apoptosis of Mouse ESCs

It has been shown that withdrawal of LIF induces mouse ESC differentiation and apoptosis (Duval et al., 2006). Mouse R1 ESCs cultured in the absence of LIF for 72 hr underwent differentiation demonstrated by AP staining (Figure 5A). We therefore examined the expression of proteins associated with pluripotency (Nanog, Oct4) and apoptosis (p53, p73, and cleaved caspase-3). As shown in Figure 5B, LIF withdrawal induced differentiation as indicated by downregulation of Oct4 and Nanog. Cleaved caspase-3, a marker of apoptosis, also increased. Interestingly, while p53 protein levels remained the same, in keeping with a recent report that p53 protein levels are unchanged during differentiation in human ESCs (Setoguchi et al., 2016), the levels of p73, RB, and cleaved caspase-3 were significantly increased (Figures 5B and S5). Similar observations were evident in AB2.2 mouse ESCs under similar experimental settings (Figure S5).

To investigate the role of p53 and/or p73 in differentiation-induced apoptosis in mouse ESCs, we examined the expression of apoptosis-associated PUMA and cleaved caspase-3 in control cells (sh-GFP), with p53 knockdown (sh-p53-1 or sh-p53-2), p73 knockdown (sh-p73-1, or sh-p73-2), or with double knockdown of p53 and p73 (sh-p53-1 and sh-p73-1). As shown in Figure 5C, again, upon LIF withdrawal, protein levels of p73, PUMA, and cleaved caspase-3 were increased significantly, whereas

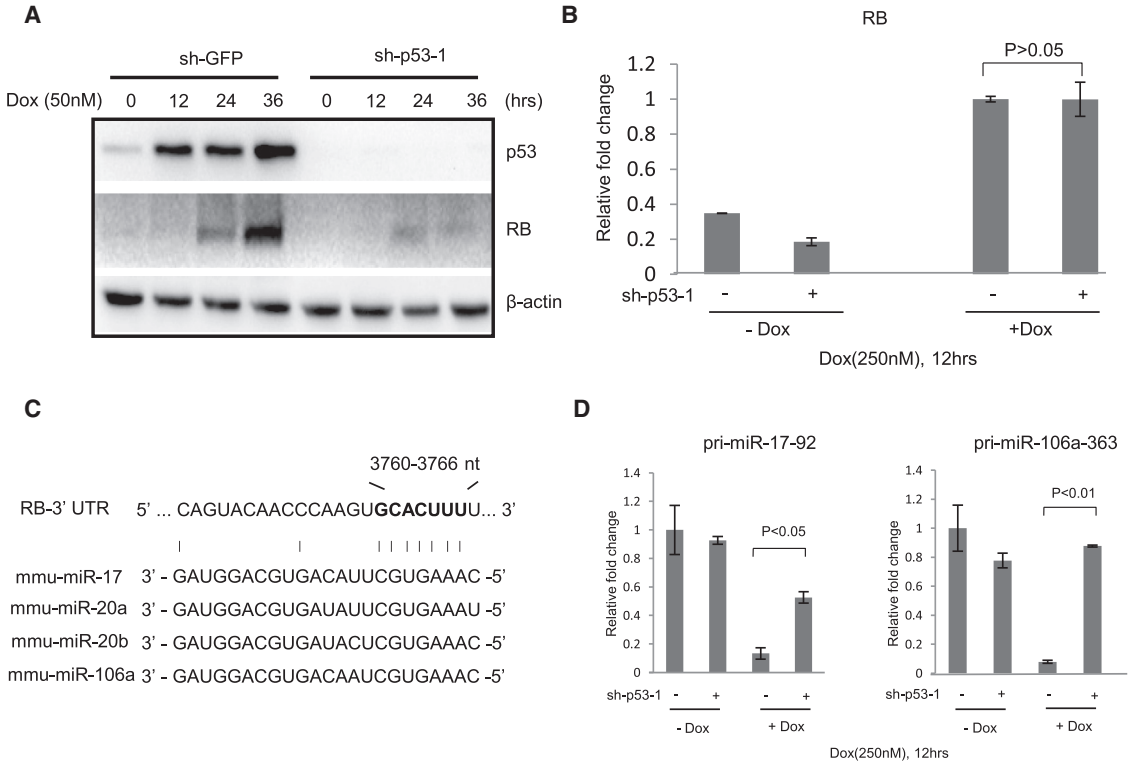

Figure 4. Doxorubicin Induces RB Protein Expression in R1 Cells in a p53-Dependent Manner

(A) R1 sh-GFP and R1 sh-p53-1 cells were treated with 50 nM doxorubicin for 12, 24, or 36 hr and were then subjected to western blot analyses.

(B) R1 sh-GFP and R1 sh-p53-1 cells were treated with or without 250 nM doxorubicin for 12 hr. Relative mRNA levels of RB were determined by qPCR. The steady-state levels of mRNA changes (fold) were calculated using the $-\Delta\Delta C_t$ method and normalized using β-actin as a control. The mean of three independent experiments in triplicate are presented. Error bars represent SEM.

(C) Schematic representation of the 3′ UTR sequence of mouse RB1 indicating the putative miRNA-binding sites (shown in bold). Four putative microRNAs are shown.

(D) R1 sh-GFP and R1 sh-p53-1 cells were treated with or without 250 nM doxorubicin for 12 hr. Expression levels of pri-miR-17-92 and pri-miR-106a-363 were analyzed by qPCR using EvaGreen and normalized to β-actin. The mean of three independent experiments in triplicate are presented. Error bars represent SEM.

the p53 protein level did not change. Unlike doxorubicin-induced p73 upregulation, which is dependent on p53, LIF-withdrawal-mediated upregulation of p73 protein was p53 independent. Furthermore, single knockdown of p53 or p73, alone, led to dramatically reduced expression of PUMA and cleaved caspase-3, whereas simultaneous knockdown of p53 and p73 completely abolished apoptosis, which was further supported by the data from the FACS analyses (Figure 5D). Together, these results indicate that p53 or p73 possesses the overlapping function in promoting differentiation-associated apoptosis.

DISCUSSION

ESCs have the ability to proliferate indefinitely in vitro. Underlying this remarkable ability are inextricably linked molecular regulatory networks such as the c-MYC and PI3K signaling pathways. However, it is not entirely clear how ESCs maintain their genome stability under stressed conditions such as DNA damage.

In this study, we investigated the role of p53, which plays a key role in guarding genome stability, in ESCs. Consistent with a previous report that p53 is important for Adriamycin (a trade name of doxorubicin)-induced apoptosis in mouse ESCs (Li et al., 2015), we found that doxorubicin or CDDP robustly activates p53/p73/RB, and cells were arrested at G2/M followed by massive apoptosis in mouse ESCs. Notably, chemical inhibition of CDK1 in ESCs can trigger DNA damage, leading to G2/M arrest and subsequent apoptosis (Huskey et al., 2015). This observation is consistent with our results that G2/M arrest precedes apoptosis. We demonstrate that both p53 and p73 play a pivotal role in promoting apoptosis induced either by DNA

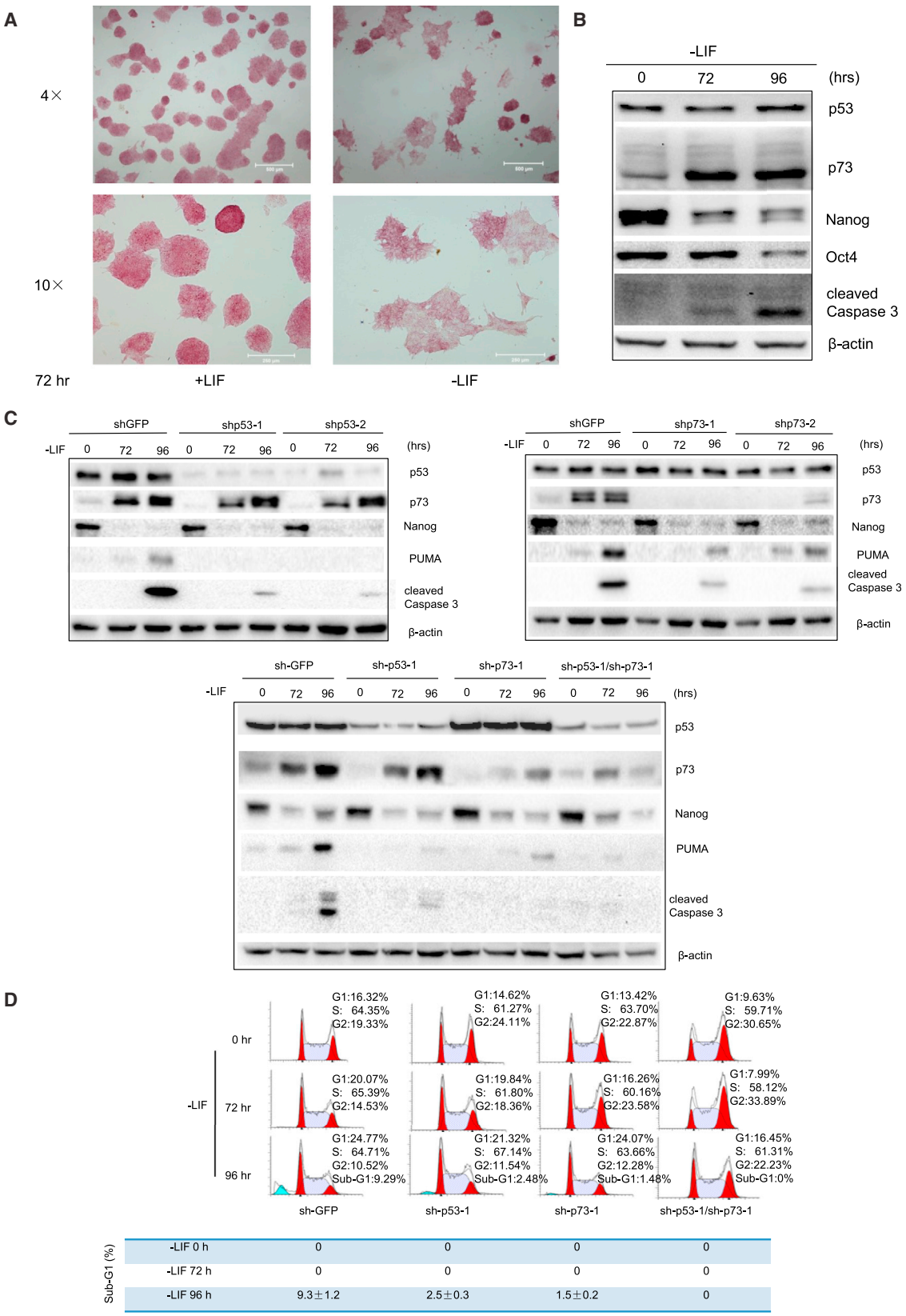

Sub-G1 (%)

-LIF 0 h	0	0	0	0
-LIF 72 h	0	0	0	0
-LIF 96 h	9.3±1.2	2.5±0.3	1.5±0.2	0

(legend on next page)

damage or by differentiation, whereas they are dispensable in cell-cycle G2M arrest in mouse ESCs in response to DNA damage.

Our study showed that neither p53 nor p73 nor RB is responsible for G2/M arrest induced by DNA damage. Although we do not know the exact mechanism for doxorubicin/CDDP-induced G2M arrest, we show that inhibition of ATM did not affect doxorubicin-induced G2/M arrest, suggesting that ATM signaling is dispensable for this process. Since CDK1 is a well-established master regulator of G2/M, it is possible that critical cell-cycle regulators, such as CDK1 or CDC25, also play a critical role in G2/M arrest in response to doxorubicin/CDDP treatment. Since the cell cycle in ESCs is unique, it seems that ESCs may use a novel checkpoint pathway(s) to monitor DNA damage to control cell-cycle progression in maintaining its genome integrity. It will be of interest to identify this novel pathway in future studies.

ESCs can differentiate into a variety of somatic cells in vitro, providing an excellent system to dissect molecular mechanisms under various cellular contexts. We show that both TAp73 and ΔNp73, two isoforms transcribed from the *Trp73* gene using alternative transcription start sites, are upregulated in a p53-dependent manner upon doxorubicin treatment in ESCs, in keeping with a report that p53 can bind the promoter of ΔNp73 (Murray-Zmijewski et al., 2006). Previous studies have shown that TAp73 promotes apoptosis, whereas ΔNp73 functions as a dominant-negative inhibitor of p53 and inhibits TAp73 transcriptional activity to attenuate apoptosis. In this study, we found that p53-induced TAp73 is largely responsible for doxorubicin-induced apoptosis in mouse ESCs, while ectopic expression of ΔNp73 suppresses this process. Strikingly, we found that induction of p73 upon ESC differentiation is independent of p53. Thus, the molecular pathway in the regulation of p73 is different upon DNA damage or upon differentiation in mouse ESCs. Consistently, knockdown of p53 alone (and thus reduction of p73 expression) is sufficient to block doxorubicin-induced apoptosis, while simultaneous knockdown of both p53 and p73 completely abolishes differentiation-induced apoptosis. It is plausible that regulation of p73 during differentiation using a p53-independent pathway may be because p73 functions in developmental processes such as neurogenesis. It will be of interest to investigate how p73 is regulated during differentiation, and how this molecular pathway overrides the regulation by p53.

Surprisingly, we found that activation of p53 led to a significant increase in RB protein expression in response to DNA damage in mouse ESCs, likely via p53-dependent suppression of *miR-17-92* and *miR-106a-363* cluster expression, which target to and inhibit RB expression. Previous studies have shown that RB does not seem to be functional in affecting cell-cycle progression in ESCs, presumably due to its hyper-phosphorylation, but RB is important for proper differentiation (Conklin et al., 2012). Thus, we suspect that RB induction by p53 sets up a cellular environment favorable to differentiation. More studies are needed to dissect the underlying mechanisms.

In summary, we demonstrate that p53 and p73 are major players in the regulation of apoptosis in mouse ESCs upon DNA damage or differentiation, indicating that p53 safeguards ESC genome stability by eliminating damaged cells. We also show that ESCs are an excellent experimental system to discover novel molecular mechanisms regarding the regulation of p73 and RB. We anticipate that understanding the difference and similarities between ESCs and cancer cells will be of value to regenerative medicine and to cancer biology.

EXPERIMENTAL PROCEDURES

Cell Culture and Drug Treatment

R1 mouse ESCs and AB2.2 mouse ESCs were cultured in DMEM (Hyclone), 15% embryonic stem screened fetal bovine serum (Hyclone), 1 mM L-glutamine, 1% non-essential amino acids, 0.1 mM β-mercaptoethanol, 1% penicillin G/streptomycin sulfate (all from Invitrogen) and 1,000 U/ml LIF (Millipore) at 37°C in a humidified 5% CO_2 incubator. Cells cultured in 2i/LIF were maintained in N2/B27 media, consisting of 50% DMEM/F12 (1:1) and 50% Neurobasal plus 0.5× N-2 supplement, 0.5× B-27 supplement, 1× penicillin/streptomycin, 1× Glutamax and 1× non-essential amino acids (NEAA) (all from Gibco), and 1× β-Me (Millipore) supplemented with 1 μM MEK inhibitor PD0325901 (Gene Operation), 3 μM GSK3 inhibitor CHIR99021 (Gene Operation), and 1,000 U/ml LIF(Millipore). Doxorubicin and CDDP were purchased from Sigma.

Figure 5. Differentiation-Induced Apoptosis of R1 Cells

(A) R1 cells were cultured in the absence of LIF for 72 hr followed by AP staining. Representative images were captured by phase-contrast microscopy.

(B) R1 cells were cultured in the absence of LIF for 72 or 96 hr. Cells were then subjected to western blot analyses. β-Actin served as a loading control.

(C and D) R1 sh-GFP, R1 sh-p53-1, R1 sh-p53-2, R1 sh-p73-1, R1 sh-p73-2, and R1 sh-p53-1/sh-p73-1 cells were cultured in the absence of LIF for 72 or 96 hr. Cells were subjected to western blot (C) or FACS analyses (D). At least three independent experiments were performed. Representative histograms and western blot data are shown.

See also Figure S5.

Western Blot Analysis

Cells were collected, washed with PBS, and re-suspended in EBC 250 lysis buffer (50 mM Tris–HCl [pH 8.0], 250 mM NaCl, 0.5% Nonidet P-40, 50 mM NaF, and 0.5 mM Na_3VO_4, 0.2 mM PMSF, 2 μg/mL leupeptin, 2 μg/mL aprotinin). Protein concentration was determined using the Bio-Rad protein assay reagent (Bio-Rad). An equal amount of protein (about 40–60 μg total protein) was loaded, separated on 10% SDS-PAGE, transferred to polyvinylidene difluoride membrane (Bio-Rad), and hybridized to an appropriate primary antibody and horseradish-peroxidase-conjugated secondary antibody for subsequent detection by ECL (Millipore). Monoclonal antibody 1C12 specific for p53 (Cell Signaling Technology) was used at a dilution of 1:1000, and phospho-p53 polyclonal antibody (#9284S, Cell Signaling Technology) was used at 1:500. Rabbit monoclonal antibody specific for p73 (#1636-1, Epitomics) and mouse monoclonal antibody specific for RB (#554136, BD) or for Oct4 (Zen BioScience) were used at 1:1,000. Polyclonal antibody specific for Nanog (A300-397, Bethyl) was used at a dilution of 1:3,000. Polyclonal antibodies for caspase-3 (#9661, Cell Signaling Technology) or PUMA (#7467, Cell Signaling Technology) were used at 1:1,000. Goat polyclonal antibody specific for actin (C-11, Santa Cruz Biotechnology) was used at 1:500.

Constructs

The shRNA constructs specific for p53, p73, and RB were generated as described (Blais et al., 2007; Johnson et al., 2007; Kawamura et al., 2009). pLVX-shRNA1 vector was obtained from Clontech. sh-p53-1 and sh-p53-2 against p53, sh-p73-1 and sh-p73-2 against pan p73, sh-RB against RB, or sh-GFP control were inserted into pLVX-shRNA1 and confirmed by DNA sequencing.

The target sequences of all these shRNAs are listed as follows:

sh-p53-1: 5′-GTACATGTGTAATAGCTCC-3′
sh-p53-2: 5′-CCGACCTATCCTTACCATCAT-3′
sh-p73-1: 5′-GGGACTTCAATGAAGGACA-3′
sh-p73-2: 5′-TGAGATCTTGATGAAAGTCAA-3′
sh-RB: 5′-GCATATCTCCGACTAAATA-3′
sh-GFP: 5′-GAAGCAGCACGACTTCTTC-3′

For overexpression experiments, full-length human ΔNp73α cDNA was sub-cloned into lentiviral vector pLVX-hPGK-puro, derived from pLVX-IRES ZsGreen1, followed by DNA sequence confirmation.

Lentiviral Infection

HEK293T cells were transfected with overexpression or shRNA constructs (and their vector controls) along with pSPAX2 and pMD2.G lentiviral packaging plasmids using lipofectamine 2000. At 48 hr after transfection, the media were collected, and cells were refed with growth media for another 24 hr. The combined media were filtered through a 0.45 μm filter to remove debris. The lentiviral particles were then concentrated by ultra-centrifugation (20,000 rpm, 2.5 hr at 4°C), re-suspended in fresh mouse ESC medium at 4°C and put on ice at least for 4 hr, and then supplemented with polybrene (10 μg/mL) and used to infect cells. Forty-eight hours after infection, the cells were selected in growth medium supplemented with puromycin (2 μg/mL) for 48 hr.

RNA Isolation and PCR Assays

Total RNA was isolated using Trizol reagent (Invitrogen) according to the manufacture's protocol. cDNA was created by using total RNA as template in the 20 μL cDNA synthesis reaction mixture containing random primers and reverse transcriptase (SuperScript II; Invitrogen) at 42°C for 1 hr, followed by 15 min of denaturation at 70°C and then quick cooling. qPCR was performed in a CFX96 Real-time PCR system (Bio-Rad) using a SoFast EvaGreen Supermix (Bio-Rad). The reactions were incubated in 96-well plates for 10 min, followed by 40 cycles of 95°C for 15 s, 60°C for 30 s. β-Actin or GAPDH was used as an endogenous control for normalization. Primer sequences are follows:

p21 Fwd, CGAGAACGGTGGAACTTTGACTTC
p21 Rev, AGAGTGCAAGACAGCGACAAGG
MDM2 Fwd, TGAGGAGGACAGCGAGGAGAAG
MDM2 Rev, CCAGTCTTGCCGTGAACAATGC
Nanog Fwd, AGTACCTCAGCCTCCAGCAGATG
Nanog Rev, GCTTCCAGATGCGTTCACCAGAT
TAp73 Fwd, GCACCTACTTTGACCTCCCC
TAp73 Rev, GCACTGCTGAGCAAATTGAAC
ΔNp73 Fwd, ATGCTTTACGTCGGTGACCC
ΔNp73 Rev, GCACTGCTGAGCAAATTGAAC
RB Fwd, ACCTTGAACCTGCTTGTCCTCT
RB Rev, GGCTGAGGCTGCTTGTGTCT
Pri-miR-17-92 cluster Fwd, CAAAGTGCTTACAGTGCAGGTAG
Pri-miR-17-92 cluster Rev, TATCTGCACTAGATGCACCTTA
Pri-miR-106a-363 cluster Fwd, GCCATCTGTGCGGTATGTGAAG
Pri-miR-106a-363 cluster Rev, GCCACTCGGAAGGTCTCTATGT
β-actin Fwd, TCACTATTGGCAACGAGCGGTTC
β-actin Rev, GCACTGTGTTGGCATAGAGGTCTT
GAPDH Fwd, TGTGTCCGTCGTGGATCTGA
GAPDH Rev, CCTGCTTCACCACCTTCTTGA

FACS Analyses

Cells were trypsinized, washed with cold PBS, and fixed in 70% ethanol at 4°C overnight. Cells (1×10^6) were stained with 50 μg/mL propidium iodide supplemented with 80 μg/mL RNase A at room temperature in the dark for 1 hr. Cells were then subjected to FACS analysis by FACScan flow cytometer (Becton Dickson). Data were analyzed using the Cell Quest program.

Procedure of Mouse ESC Differentiation

R1 cells or AB2.2 cells were plated at low cell density (1×10^5 cells/well in a six-well plate) in mouse ESC medium containing LIF (1,000 U/ml). Twelve hours after seeding, cells were washed once with PBS at room temperature and fed with mouse ESC medium supplemented with or without mLIF. The medium was changed every 24 hr, and cells were collected at an indicated time (3 or 4 days).

Alkaline Phosphatase Staining Assay

Cells were washed once with PBS and fixed in 3.7% formaldehyde for 5 min at room temperature. Cells were then incubated with AP staining buffer (FRV-Alkaline solution/sodium nitrite solution/naphthol AS-BI alkaline solution; Sigma) at room temperature for 10–30 min. Images of the stained cells were captured with a Nikon (ECLIPSE Ti-U) reverse phase-contrast microscope.

SUPPLEMENTAL INFORMATION

Supplemental Information includes five figures and can be found with this article online at http://dx.doi.org/10.1016/j.stemcr.2016.10.008.

AUTHOR CONTRIBUTIONS

H.H. performed the experiments in Figures 1, 2, 3, 4, and S3. C.W. performed the experiments in Figures 3, 4, 5, S1, S2, and S5. Q.D. and F.L. performed the experiments including Figures 5 and S4. J.B. and Z.L. contributed to the experimental design. Z.-X.X. and Q.L. designed the study and wrote the manuscript. All authors reviewed the manuscript.

ACKNOWLEDGMENTS

We thank members of the Xiao Lab for many stimulating discussions. We thank Kang Han for technical help on FACS, qPCR, and microscope work. This study was supported by the National Key Basic Research Program (973 Program) of China (2012CB910700) to Z.X.; National Natural Science Foundation of China (NSFC) grants to Z.X. (81330054 and 81520108020) and to Q.L. (81671115); Science and Technology Department of Sichuan Province to Z.X. (2014SZ0116) and to Q.L. (2016JQ0029), and the Ministry of Education of China to Q.L. (PCSIRT0935).

Received: May 12, 2016
Revised: October 21, 2016
Accepted: October 24, 2016
Published: November 17, 2016

REFERENCES

Aladjem, M.I., Spike, B.T., Rodewald, L.W., Hope, T.J., Klemm, M., Jaenisch, R., and Wahl, G.M. (1998). ES cells do not activate p53-dependent stress responses and undergo p53-independent apoptosis in response to DNA damage. Curr. Biol. *8*, 145–155.

Blais, A., van Oevelen, C.J., Margueron, R., Acosta-Alvear, D., and Dynlacht, B.D. (2007). Retinoblastoma tumor suppressor protein-dependent methylation of histone H3 lysine 27 is associated with irreversible cell cycle exit. J. Cell Biol. *179*, 1399–1412.

Chao, C., Saito, S., Anderson, C.W., Appella, E., and Xu, Y. (2000). Phosphorylation of murine p53 at ser-18 regulates the p53 responses to DNA damage. Proc. Natl. Acad. Sci. USA *97*, 11936–11941.

Conklin, J.F., Baker, J., and Sage, J. (2012). The RB family is required for the self-renewal and survival of human embryonic stem cells. Nat. Commun. *3*, 1244.

de Vries, A., Flores, E.R., Miranda, B., Hsieh, H.M., van Oostrom, C.T., Sage, J., and Jacks, T. (2002). Targeted point mutations of p53 lead to dominant-negative inhibition of wild-type p53 function. Proc. Natl. Acad. Sci. USA *99*, 2948–2953.

Duval, D., Trouillas, M., Thibault, C., Dembele, D., Diemunsch, F., Reinhardt, B., Mertz, A.L., Dierich, A., and Boeuf, H. (2006). Apoptosis and differentiation commitment: novel insights revealed by gene profiling studies in mouse embryonic stem cells. Cell Death Differ. *13*, 564–575.

Freed-Pastor, W.A., and Prives, C. (2012). Mutant p53: one name, many proteins. Genes Dev. *26*, 1268–1286.

Hickson, I., Zhao, Y., Richardson, C.J., Green, S.J., Martin, N.M., Orr, A.I., Reaper, P.M., Jackson, S.P., Curtin, N.J., and Smith, G.C. (2004). Identification and characterization of a novel and specific inhibitor of the ataxia-telangiectasia mutated kinase ATM. Cancer Res. *64*, 9152–9159.

Hong, Y., and Stambrook, P.J. (2004). Restoration of an absent G1 arrest and protection from apoptosis in embryonic stem cells after ionizing radiation. Proc. Natl. Acad. Sci. USA *101*, 14443–14448.

Huskey, N.E., Guo, T., Evason, K.J., Momcilovic, O., Pardo, D., Creasman, K.J., Judson, R.L., Blelloch, R., Oakes, S.A., Hebrok, M., et al. (2015). CDK1 inhibition targets the p53-NOXA-MCL1 axis, selectively kills embryonic stem cells, and prevents teratoma formation. Stem Cell Rep. *4*, 374–389.

Irwin, M., Marin, M.C., Phillips, A.C., Seelan, R.S., Smith, D.I., Liu, W., Flores, E.R., Tsai, K.Y., Jacks, T., Vousden, K.H., et al. (2000). Role for the p53 homologue p73 in E2F-1-induced apoptosis. Nature *407*, 645–648.

Isobe, M., Emanuel, B.S., Givol, D., Oren, M., and Croce, C.M. (1986). Localization of gene for human p53 tumour antigen to band 17p13. Nature *320*, 84–85.

Johnson, J., Lagowski, J., Sundberg, A., Lawson, S., Liu, Y., and Kulesz-Martin, M. (2007). p73 loss triggers conversion to squamous cell carcinoma reversible upon reconstitution with TAp73alpha. Cancer Res. *67*, 7723–7730.

Kawamura, T., Suzuki, J., Wang, Y.V., Menendez, S., Morera, L.B., Raya, A., Wahl, G.M., and Izpisua Belmonte, J.C. (2009). Linking the p53 tumour suppressor pathway to somatic cell reprogramming. Nature *460*, 1140–1144.

Kruse, J.P., and Gu, W. (2009). Modes of p53 regulation. Cell *137*, 609–622.

Li, M., Gou, H., Tripathi, B.K., Huang, J., Jiang, S., Dubois, W., Waybright, T., Lei, M., Shi, J., Zhou, M., et al. (2015). An apela RNA-containing negative feedback loop regulates p53-mediated apoptosis in embryonic stem cells. Cell Stem Cell *16*, 669–683.

Lin, T., Chao, C., Saito, S., Mazur, S.J., Murphy, M.E., Appella, E., and Xu, Y. (2005). p53 induces differentiation of mouse embryonic stem cells by suppressing Nanog expression. Nat. Cell Biol. *7*, 165–171.

Mendell, J.T. (2008). miRiad roles for the miR-17-92 cluster in development and disease. Cell *133*, 217–222.

Momcilovic, O., Choi, S., Varum, S., Bakkenist, C., Schatten, G., and Navara, C. (2009). Ionizing radiation induces ataxia telangiectasia mutated-dependent checkpoint signaling and G(2) but not G(1) cell cycle arrest in pluripotent human embryonic stem cells. Stem Cells *27*, 1822–1835.

Murray-Zmijewski, F., Lane, D.P., and Bourdon, J.C. (2006). p53/p63/p73 isoforms: an orchestra of isoforms to harmonise cell differentiation and response to stress. Cell Death Differ. *13*, 962–972.

Nakagawa, T., Takahashi, M., Ozaki, T., Watanabe Ki, K., Todo, S., Mizuguchi, H., Hayakawa, T., and Nakagawara, A. (2002).

Autoinhibitory regulation of p73 by Delta Np73 to modulate cell survival and death through a p73-specific target element within the Delta Np73 promoter. Mol. Cell. Biol. *22*, 2575–2585.

Qi, Y., Qiu, Q., Gu, X., Tian, Y., and Zhang, Y. (2016). ATM mediates spermidine-induced mitophagy via PINK1 and Parkin regulation in human fibroblasts. Sci. Rep. *6*, 24700.

Qin, H., Yu, T., Qing, T., Liu, Y., Zhao, Y., Cai, J., Li, J., Song, Z., Qu, X., Zhou, P., et al. (2007). Regulation of apoptosis and differentiation by p53 in human embryonic stem cells. J. Biol. Chem. *282*, 5842–5852.

Sayan, B.S., Yang, A.L., Conforti, F., Tucci, P., Piro, M.C., Browne, G.J., Agostini, M., Bernardini, S., Knight, R.A., Mak, T.W., et al. (2010). Differential control of TAp73 and DeltaNp73 protein stability by the ring finger ubiquitin ligase PIR2. Proc. Natl. Acad. Sci. USA *107*, 12877–12882.

Setoguchi, K., TeSlaa, T., Koehler, C.M., and Teitell, M.A. (2016). P53 regulates rapid apoptosis in human pluripotent stem cells. J. Mol. Biol. *428*, 1465–1475.

Silva, J., Nichols, J., Theunissen, T.W., Guo, G., van Oosten, A.L., Barrandon, O., Wray, J., Yamanaka, S., Chambers, I., and Smith, A. (2009). Nanog is the gateway to the pluripotent ground state. Cell *138*, 722–737.

Smith, A.G. (2001). Embryo-derived stem cells: of mice and men. Annu. Rev. Cell Dev. Biol. *17*, 435–462.

Vousden, K.H., and Prives, C. (2009). Blinded by the light: the growing complexity of p53. Cell *137*, 413–431.

Ying, Q.L., Wray, J., Nichols, J., Batlle-Morera, L., Doble, B., Woodgett, J., Cohen, P., and Smith, A. (2008). The ground state of embryonic stem cell self-renewal. Nature *453*, 519–523.